Multielement Determination of Trace Elements in Sediment Sample by Inductively Coupled Plasma Mass Spectrometry with Microsampling Technique

Eiji Fujimori, Rong Wei, Hideyuki Sawatari, Koichi Chiba, and Hiroki Haraguchi*

Department of Applied Chemistry, School of Engineering, Nagoya University, Furo-cho, Chikusa-ku, Nagoya 464-01

(Received July 25, 1996)

A discrete microsampling technique for multielement determination of trace elements by inductively coupled plasma mass spectrometry has been investigated for analyses of samples containing large amounts of matrix elements. In the technique, 100 μl of the sample solution was introduced into the plasma by using a six-way valve, and 10 elements were detected in peak hopping mode during a single mass range scan. As a result, a transient peak profile of the signal for each element was observed at each *m/z* position. The peak area measurement method was established for the quantitative analysis. The optimization of instrumental conditions and matrix effects in multielement determination were investigated in detail. The discrete microsampling technique was found to reduce some memory effects due to matrices in ICP-MS. The present system was applied to the analyses of standard sediment sample and 30 elements at the $\mu g\,g^{-1}$ level were successfully determined without matrix separation.

In recent years, inductively coupled plasma mass spectrometry (ICP-MS) has been becoming one of the most convenient analytical methods for the determination of trace elements in various kinds of sample.[1,2] ICP-MS provides many excellent analytical features such as low detection limits at the $pg\,ml^{-1}$ level for many elements, wide dynamic range of calibration curve ($ng\,ml^{-1}$—$pg\,ml^{-1}$), and multielement detection capability. However, there is some difficulty in introduction of the samples with a large amount of concomitant salts,[3] which cause matrix effects, memory effects, and clogging of a plasma torch and a sampling orifice to result in instrumental drift, as well as signal suppression or enhancement. In conventional continuous nebulization, 2—3 ml portion of the sample solution is generally introduced into a plasma in one measurement, and thus a large amount of concomitant salts is inevitably introduced into the ICP-MS instrument. Common alternatives to avoid matrix effects are dilution of samples or separation of analytes from matrices. However, large dilution of the sample causes the difficulty in the determination of analyte elements at the trace and ultratrace levels, and further complicated sample pretreatment involves some risks of contamination.

Flow injection (FI)-ICP-MS have been examined by many works for the purpose of performing an on-line sample pretreatment just before sample introduction.[4—8] Standard addition,[4,5] isotope dilution,[6] ion-exchange[7,8] have been adopted in flow injection technique for on-line procedures. In addition, flow injection also helps to alleviate some of the problems caused by matrix elements, because an injected sample is substantially diluted in long tubing of a flow injection system by dispersion.[9,10]

Recently, the present authors also reported a preliminary study on the discrete microsampling technique for multielement detection by ICP-MS[11], where a small amount of sample was discretely introduced into ICP-MS. By using this technique, the instrument was not exposed to massive amounts of matrix elements, even when highly concentrated samples were analysed. In the present experiment, hence, simultaneous multielement determination of trace elements by microsampling ICP-MS has been further investigated, along with optimization of instrumental conditions and effect of matrix elements. In addition, this system was applied to the determination of 30 trace elements in the sediment standard sample.

Experimental

Instrumentation. The ICP-MS instrument used was model SPQ 8000 from Seiko Instrument Co.(Tokyo, Japan). For discrete microsampling introduction, the sample introduction system was constructed by using a six-way valve (Teflon rotary valve Type 50, Rheodyne, Cotati, CA, USA), a 100 μl sample loop and a peristaltic pump (Model Minipuls 2 ; Gilson, Villiers le Bel, France). The six-way valve and the nebulizer was connected with a piece of Teflon® tubing. The details of the introduction system were described in the previous paper.[11] The carrier solution was supplied continuously to the nebulizer through the six-way valve by the peristaltic pump (hereafter, the flow rate of the carrier solution is defined as the "flow rate") and 100 μl of the sample solution loaded in a sample loop was led to the nebulizer by switching the valve position of the six-way valve manually. Data accumulation was carried out according to the program for a device of electrothermal vaporization / ICP-MS (Seiko Instrument Co.). The instrumental components and operational conditions of ICP-MS are summarized in Table 1. An ICP-AES (inductively coupled plasma atomic emission spectrometry) instrument of model Plasma AtomComp MK II

Table 1. Instrumental Components and Operating Conditions of ICP-MS

Plasma conditions	
RF frequency	27.12 MHz
Incident power	1.2 kW
Coolant Ar gas	16 l min^{-1}
Auxiliary Ar gas	1.0 l min^{-1}
Carrier Ar gas	0.5 l min^{-1} (2.5 kgf cm^{-2})
Nebulizer	Glass concentric type (Meinhard TR-30-A2)
Sampling conditions	
Sampling cone	Copper 1.1 mmϕ
Skimmer cone	Copper 0.35 mmϕ
Sampling depth	9 mm from work coil
Data acquisition	Peak hopping mode
Dwell time/peak	10 ms
Number of isotopes/scan	6—10
Number of scans	max. 500 times
Data acquisition time	85 s

(Jarrell-Ash, Franklin, MA, USA) was used for the determination of major elements in the sediment sample.

Chemicals. High-purity water was prepared by a Millipore Milli-Q water purification system (receptivity of 18 MΩ cm^{-1}; Millipore Kogyo Co., Tokyo, Japan). Nitric acid, hydrofluoric acid and perchloric acid of analytical regent grade were purchased from Wako Pure Chemical Industries Ltd. (Osaka, Japan), and lithium metaborate ($LiBO_2$) of Suprapur® grade was from Merck (Dortmund, Germany). The multielement standard solutions were prepared by mixing aliquots of 1000 μg ml^{-1} of the single-element stock solutions for atomic absorption spectrometry in 0.1 M of nitric acid solution (1 M= 1 mol dm^{-3}). The acid concentration of the carrier solution was adjusted to that of the standard solutions.

Sample Preparation. The sediment standard sample JLk-1 (lake sediment) issued from the Geological Survey of Japan (Tsukuba) was decomposed by two methods : alkali fusion and acid digestion. In alkali fusion, ca. 0.2 g of the sample was decomposed with ca. 0.3 g of $LiBO_2$ and diluted with 1 M HNO_3 to 100 ml. In acid digestion, ca. 0.2 g of the sample was decomposed with hydrofluoric, nitric, and perchloric acids, and finally diluted to 100 ml with water. The decomposed solutions were further diluted by 5-fold, after internal standard elements (In, Re, and Bi; 10 ng ml^{-1} each) were added to them.

Measurement Procedure. At most 10 elements (isotopes) including internal standard elements were measured simultaneously in one sample injection. In each measurement, two of In, Re, or Bi were selected as the internal standard elements, depending on the mass range of the analyte elements. Thirty elements in the sediment sample were determined by four injections.

Results and Discussion

Dependence of Signal Intensities on the Flow Rate of Carrier Solution and Nebulizer Gas Pressure. In discrete microsampling technique, the transient signals were observed, and they were significantly influenced by the flow rate of the carrier solution introduced into the six-way valve. Thus, dependence of the signal profiles and intensities on the flow rate of the carrier solution were investigated first. A mixture of Ni, Ge, Mo, In, Ce, and Bi (100 ng ml^{-1} each) was used in the experiment. The signal profiles obtained by the present microsampling system are shown in Fig. 1. As is seen in Fig. 1, the broad signal profiles were observed at the low flow rate of the carrier solution. On the other hand, the signal profiles became sharper and higher at the higher flow rate, although the maximum peaks were not always observed at the highest flow rate. The effects of the flow rates on signal peak areas and heights are summarized in Fig. 2. The peak areas for all elements were diminished with increasing the flow rate. Such effects have been well characterized in flow injection atomic absorption spectrometry.[12] On the other hand, the signal peak heights showed different behaviors, that is, maximum peak heights of the individual elements were observed at the different flow rates. As the compromised conditions for simultaneous multielement detection in the present experiment, 1.0 ml min^{-1} of the flow rate was chosen to obtain relatively large peak height intensities for all elements as well as peak area intensities.

Nebulizer gas pressure for sample nebulization (uptake) into the plasma also gives great influence on the profiles of the transient signals in microsampling ICP-MS. Thus, the effect of nebulizer gas pressure on the signal peak area and peak height was investigated, where nebulizer gas pressure was varied in the range of 2.0—2.8 kgf cm^{-2}. The results are shown in Fig. 3. As is seen in the figures, the peak areas and heights of the transient signals showed similar trends to each other. Both peak areas and heights of Bi and In simply increased with the increase of nebulizer gas pressure, while those of Ni, Ge, Mo, and Ce showed the maximum intensities at the smaller nubulizer gas pressure. The nebulizer gas pressure was set to be 2.4 kgf cm^{-2} as the compromised conditions for a variety of the elements to obtain appropriate signal intensities.

Coedo and Dorado[13] reported that the optimum nebulizer gas flow rate was mass-dependent and that the heavier elements had lower flow rate as an optimum. However, no mass-dependent tendency was observed in this experiment. First ionization energies of atoms and bond strengths of their monoxide molecules are listed in Table 2.[14] It is seen from Fig. 2(b) and Table 2 that there is a tendency that the element with large bond strength provides a maximum peak height at the lower flow rate.

Matrix Effects in Microsampling ICP-MS. The effects of matrix elements on the signal intensities are usually prone to cause sensitivity suppression as well as polyatomic interferences in ICP-MS measurement. The effect of the Na concentration on the peak areas and heights was investigated as an example. The signals of Ni, Ge, Mo, In, Ce, and Bi (10 ng ml^{-1} each) were measured under the compromised conditions of the flow rate and nebulizer gas pressure, as mentioned above. Matrix effects of Na on all the elements were almost the same in the microsampling nebulization. The matrix effects obtained in continuous nebulization ICP-MS were also investigated under the same experimental conditions. Both peak areas and peak heights of signals were suppressed with the increase of the Na concentration, and the signal suppression in the discrete microsampling technique

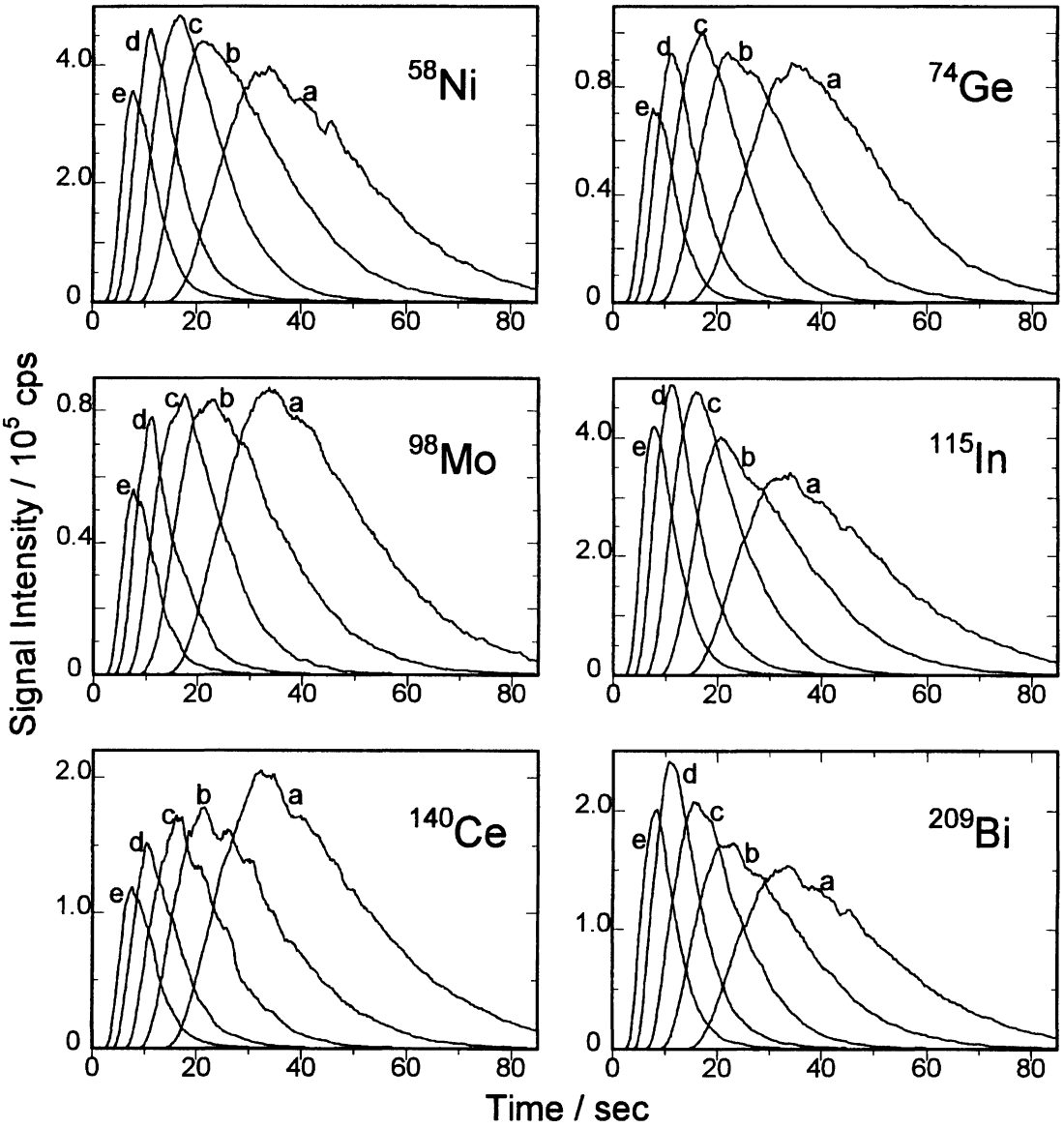

Fig. 1. Signal profiles for Ni, Ge, Mo, In, Ce, and Bi observed by microsampling ICP-MS. Flow rate of the carrier solution : a) 0.5 ml min^{-1}, b) 0.75 ml min^{-1}, c) 1.0 ml min^{-1}, d) 1.5 ml min^{-1}, e) 2.0 ml min^{-1}.

Table 2. Ionization Energy of the Elements and Bond Strength in Metal Monoxide (MO) Molecule[14)]

Element	Ionization energy[a)]	Bond strength in MO molecule
	kJ mol^{-1}	kJ mol^{-1}
Ni	736.7	382.0
Ge	762.1	659.4
Mo	684.9	560.2
In	558.3	<320.1
Ce	527.8	797
Bi	755.4	337.2

a) First ionization energies of the elements (atoms) listed.

was quite similar to that in the continuous nebulization.

The stability of measurement was also investigated to evaluate the precision of the analysis by microsampling ICP-MS. A measurement sequence of the test solution with 6 elements (Ni, Ge, Mo, In, Ce, and Bi; 10 ng ml^{-1} each) with and without matrix was performed as follows : The test solution without matrix was first measured, the solution with matrix was then measured 3 times, and the solution without matrix was measured again. In the sequential measurement, the matrix (Na) concentration was increased from Na 1 μg ml^{-1} up to 100 μg ml^{-1}. The results in the case of In are shown in Fig. 4. In the discrete microsampling measurement, the signal peak areas of the In solution without matrix (Na 0 μg ml^{-1}) were almost constant throughout the experiment, even after Na 100 μg ml^{-1} solution was introduced. On the contrary, these values obtained by the continuous nebulization method markedly varied and decreased with increase of the Na concentration. The discrete microsampling technique reduces some kinds of memory effect of matrices which suppress a measured signal, and so it is able to exclude the instability of measurement due to concomitant salts. This

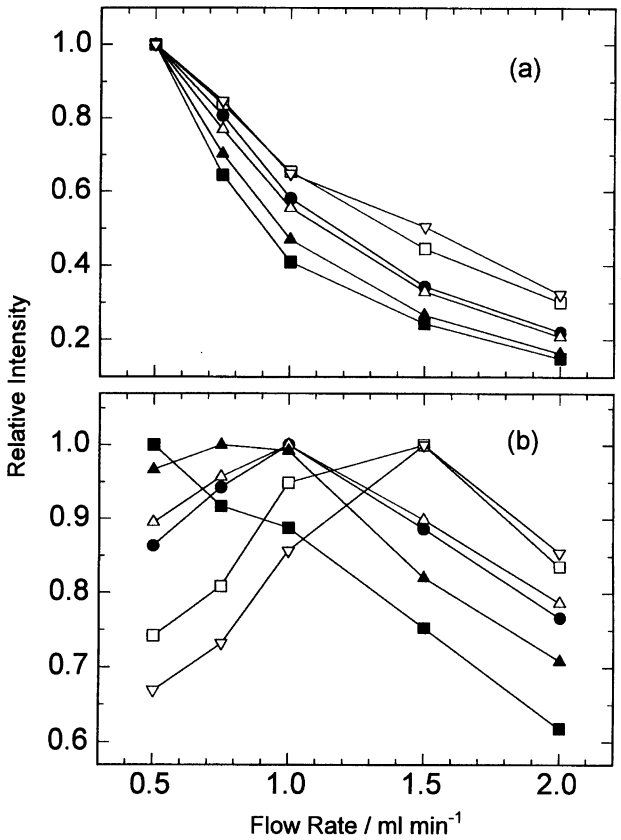

Fig. 2. Dependence of peak areas and heights of the observed signals on flow rate of the carrier solution. (a) peak area measurement, (b) peak height measurement. ●:Ni, △:Ge, ▲:Mo, □:In, ■:Ce, ▽:Bi.

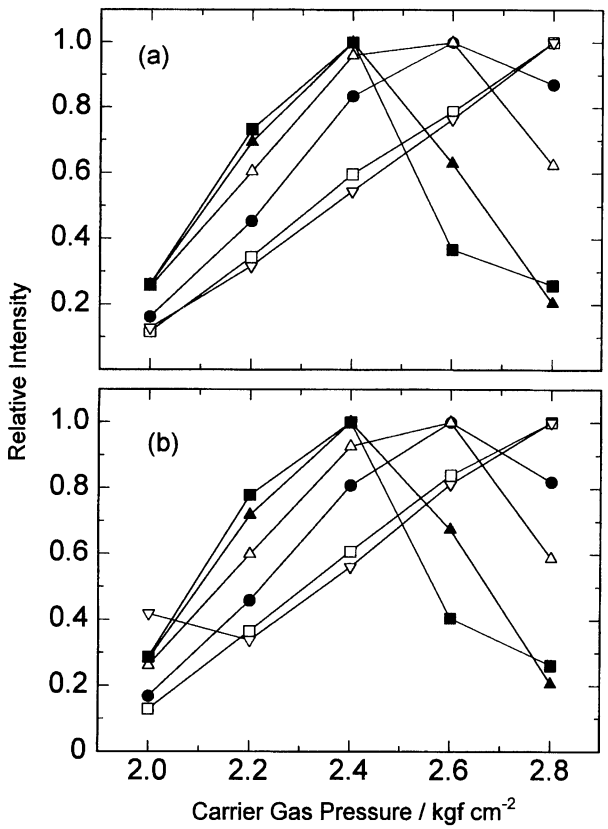

Fig. 3. Dependence of peak areas and heights of the observed signals on nebulizer gas pressure. (a) peak area measurement, (b) peak height measurement. Flow rate of the carrier solution: 1.0 ml min^{-1}. ●:Ni, △:Ge, ▲:Mo, □:In, ■:Ce, ▽:Bi.

fact suggests that the present discrete microsampling ICP-MS is preferable to conventional ICP-MS with continuous nebulization when the samples with large amounts of dissolved salts are analyzed.

Reproducibility in Analyte Signal Measurement. The reproducibilities of the peak area and the height measurements in discrete microsampling were investigated, where 100 μl of the analyte solution was injected 5-times. In this experiment, the signal peak areas and the heights of 6 elements (Ni, Ge, Mo, In, Ce, and Bi; 100 ng ml^{-1} each) were measured simultaneously. The relative standard deviations of this method are summarized in Table 3. It is noted that the peak area method provided better precision for all elements than the height method, because the measurement of a tran-

Table 3. Relative Standard Deviation (%) of Peak Area and Peak Height Measurements by Microsampling ICP-MS

Element	m/z	Peak area[a)]	Peak height[a)]
Ni	58	1.32	2.28
Ge	74	0.97	2.19
Mo	98	0.81	2.18
In	115	1.28	1.99
Ce	140	0.83	4.73
Bi	209	1.82	2.44

a) Estimated from 5-times measurements.

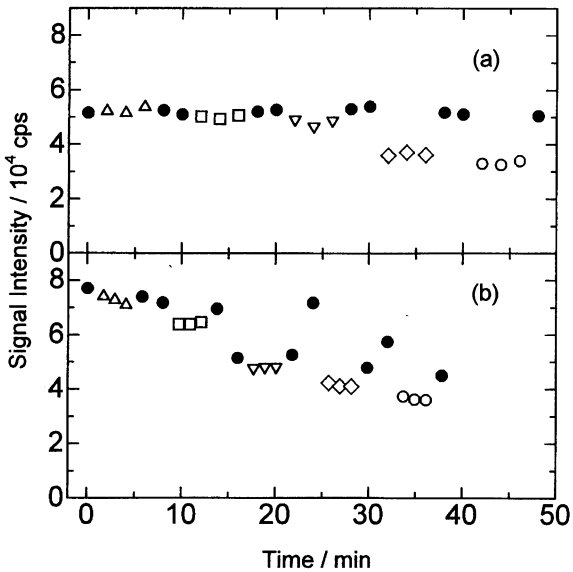

Fig. 4. Variation of signal intensities in sequential measurements. (a) Peak area measurement by microsampling ICP-MS. Flow rate of the carrier solution: 1.0 ml min^{-1}, Nebulizer gas pressure: 2.4 kgf cm^{-2}. (b) Continuous nebulization ICP-MS. Sample uptake rate: 0.7 ml min^{-1}, Nebulizer gas pressure: 2.5 kgf cm^{-2}. Concentration of Na: ● 0 μg ml^{-1}, △ 1 μg ml^{-1}, □ 5 μg ml^{-1}, ▽ 10 μg ml^{-1}, ◇ 50 μg ml^{-1}, ○ 100 μg ml^{-1}.

Table 4. Detection Limits Obtained by Microsampling and Conventional ICP-MS (unit : ng ml^{-1})

Element	m/z	Present system	Conventional nebulization	Element	m/z	Present system	Conventional nebulization
Li	7	18	1	Ag	107	0.06	0.007
Be	9	12	2	Cd	114	0.01	0.002
B	11	27	8	In	115	0.0008	0.0003
Na	23	0.3	0.08	Sn	120	0.02	0.03
Mg	24	0.6	0.1	Sb	121	0.02	0.01
Al	27	0.3	0.1	Te	130	0.09	0.01
Si	29	68	3	Cs	133	0.007	0.003
P	31	6	3	Ba	138	0.04	0.01
K	39	2	0.6	La	139	0.006	0.0007
Ca	44	3	0.3	Ce	140	0.006	0.0009
Sc	45	0.008	0.003	Pr	141	0.002	0.0003
Ti	48	0.1	0.07	Nd	146	0.01	0.004
V	51	0.02	0.009	Sm	147	0.006	0.001
Cr	52	0.06	0.006	Eu	153	0.003	0.0004
Mn	55	0.01	0.004	Gd	157	0.01	0.001
Fe	57	2	0.6	Tb	159	0.002	0.0003
Co	59	0.005	0.005	Dy	163	0.006	0.0007
Ni	60	0.01	0.007	Ho	165	0.001	0.0003
Cu	63	0.3	0.03	Er	166	0.005	0.0007
Zn	64	0.08	0.03	Tm	169	0.001	0.0002
Ga	69	0.01	0.007	Yb	174	0.005	0.0009
Ge	74	0.01	0.002	Lu	175	0.002	0.0004
As	75	0.03	0.01	W	184	0.03	0.006
Se	78	0.5	0.07	Re	187	0.003	0.0005
Rb	85	0.01	0.004	Pt	195	0.01	0.003
Sr	88	0.008	0.001	Au	197	0.09	0.005
Y	89	0.001	0.0005	Hg	202	0.7	0.1
Zr	90	0.2	0.04	Pb	208	0.05	0.02
Mo	98	0.009	0.007	Bi	209	0.005	0.0007
Rh	103	0.0009	0.0003	Th	232	0.008	0.0008
Pd	105	0.01	0.001	U	238	0.005	0.003

sient signal inevitably deteriorates the signal-to-background ratio. In consequence, the peak area method was adopted for quantitative analysis in the following.

Detection Limit. The detection limits obtained by the discrete microsampling ICP-MS are summarized in Table 4. These detection limits were estimated as the concentration of the analyte elements corresponding to 3σ (σ: standard deviation) of the background signal. In comparison, the detection limits obtained by conventional ICP-MS are also listed in Table 4. This shows that the detection limits obtained by microsampling technique were worse by several times than those obtained by the conventional method. Even so, the detection limits obtained by microsampling ICP-MS are sensitive enough to apply to trace analysis of various samples, especially, with the highly concentrated matrix elements.

Determination of Trace Elements in Sediment Sample. The present microsampling ICP-MS system was applied to the determination of trace elements in standard sediment sample (JLk-1). The major constituents in the digested sample solutions were measured by ICP-AES. Their total concentrations were about 500 $\mu g\,ml^{-1}$ in the alkali fusion solutions and about 90 $\mu g\,ml^{-1}$ in the acid digestion solution. The trace elements were measured by ICP-MS, where matrix effects were corrected by the internal standardization method.[15] The results are summarized in Table 5 together with the reference values,[16,17] where the values of major elements obtained by ICP-AES are also added. Vanadium in the acid digestion solution and Sc in the alkali fusion solution could not be determined because of the polyatomic interferences caused by $^{35}Cl^{16}O$ and $^{29}Si^{16}O$, respectively. Zirconium was determined as 68.0 $\mu g\,g^{-1}$ for the acid digestion sample solution, although it was 123 $\mu g\,g^{-1}$ for the alkali fusion sample and the reference value is 140.6 $\mu g\,g^{-1}$. This may be caused by incomplete decomposition of zircon ($ZrSiO_4$) by acid digestion.[18] It is known that zircon usually enriches heavy rare earth elements (REEs) rather than light REEs.[18] Consequently, the observed values of heavy REEs in the acid digested sample were slightly lower than those prepared by alkali fusion. In general, the observed values obtained by the different sample decomposition methods were in good agreement with the reference values. It is seen in Table 5 that 30 elements were determined by the present microsampling ICP-MS. The concentrations of other elements were too low to be determined by the microsampling technique, although the determination of Pb was not tried.

Conclusion

The discrete microsampling technique for inductively cou-

Table 5. Analytical Results for Major Composition and Trace Elements in Standard Sediment JLk-1

Composition[a]	Observed value[b]		Reference	Detection
	Alkali fusion	Acid digestion	value[c]	limit
SiO_2	59.7 ± 1.1%	–	57.50 ± 0.928%	0.03%
Al_2O_3	16.6 ± 0.4	17.0 ± 0.1%	16.81 ± 0.264	0.05
T-Fe_2O_3	6.74 ± 0.14	6.91 ± 0.05	6.98 ± 0.288	0.004
K_2O	2.8 ± 0.5	2.9 ± 0.2	2.822 ± 0.124	0.9
MgO	1.71 ± 0.01	1.76 ± 0.01	1.79 ± 0.100	0.04
Na_2O	1.06 ± 0.04	1.30 ± 0.09	1.03 ± 0.087	0.03
TiO_2	0.694 ± 0.008	0.541 ± 0.012	0.663 ± 0.031	0.002
CaO	0.69 ± 0.01	0.69 ± 0.01	0.686 ± 0.033	0.01
MnO	0.265 ± 0.002	0.270 ± 0.002	0.265 ± 0.017	0.001
P_2O_5	N. D.[d]	0.28 ± 0.08	0.213 ± 0.023	0.09
Ba	508 ±16 μg g^{-1}	524 ± 7 μg g^{-1}	586 ±55 μg g^{-1}	0.1 μg g^{-1}
Rb	133 ± 3	139 ± 3	145.8 ±14.18	0.03
V	115 ± 3	–	118.71 ±17.2	0.05
Zn	113 ± 1	119 ± 2	151.39 ±20.94	0.2
Cr	66.6 ± 0.9	57.8 ± 0.9	74.15 ±11.3	0.2
Cu	63.7 ± 7.1	57.8 ± 0.9	60.9 ± 4.1	0.8
Sr	63.1 ± 1.1	63.8 ± 1.8	71.75 ±14.577	0.02
Ni	32.0 ± 0.1	29.5 ± 0.4	34.86 ± 4.14	0.03
Co	19.3 ± 0.4	17.3 ± 0.4	16.6 ± 3.47	0.01
Th	18.2 ± 0.6	19.9 ± 0.7	19.6 ± 1.01	0.02
Cs	11.2 ± 0.6	12.1 ± 0.1	11.0 ± 1.63	0.02
U	5.17 ± 0.27	4.51 ± 0.10	3.69 ± 0.65	0.01
Mo	1.83 ± 0.06	1.59 ± 0.09	(2.05)[e]	0.02
Sc	–	14.6 ± 0.2	16.0 ± 1.2	0.02
Y	36.0 ± 1.2	30.1 ± 0.8	40.8 ± 5.1	0.003
Zr	123 ± 3	68.0 ± 6.7	146 ±15	0.5
La	35.7 ± 1.1	41.0 ± 0.7	41.3 ± 2.1	0.02
Ce	78.9 ± 2.0	86.6 ± 1.1	89.1 ± 8.1	0.02
Pr	8.95 ± 0.31	9.81 ± 0.05	8.4 ± 1.8	0.005
Nd	30.5 ± 0.4	33.7 ± 1.0	35.4 ± 3.0	0.03
Sm	6.72 ± 0.32	7.30 ± 0.23	8.0 ± 0.6	0.02
Eu	1.27 ± 0.06	1.31 ± 0.02	1.4 ± 0.1	0.008
Gd	6.20 ± 0.24	6.94 ± 0.17	4.9 ~ 6.6	0.03
Tb	0.972 ± 0.067	0.964 ± 0.029	1.3 ± 0.1	0.005
Dy	5.79 ± 0.35	5.37 ± 0.09	6.54 ± 0.6	0.02
Ho	1.19 ± 0.08	1.03 ± 0.04	1.20, 1.52	0.003
Er	3.49 ± 0.16	2.97 ± 0.12	3.5 ± 0.4	0.01
Tm	0.537 ± 0.014	0.455 ± 0.015	0.53, 0.66	0.003
Yb	3.60 ± 0.30	3.02 ± 0.03	4.1 ± 0.3	0.01
Lu	0.491 ± 0.027	0.449 ± 0.018	0.60 ± 0.07	0.005

a) The observed values of major composition (SiO_2—P_2O_5) were obtained by ICP-AES. b) Mean±s.d. (n=3). c) The reference values for SiO_2—Mo were cited from Ref. 16 and others from Ref. 17. d) Not determined. e) Information value.

pled plasma mass spectrometry was useful for the multielement determination of trace elements. This technique reduces memory effects due to concomitant salts in ICP-MS. It was applied to the analysis of a sediment sample decomposed by alkali fusion and acid digestion. Consequently, 30 elements including rare earth elements could be determined; analytical results for each sediment sample digested by both the alkali fusion and the acid digestion agreed quite well with each other and with their certified values. It is concluded that the present technique is very useful for the analysis of the solution with highly-concentrated salts as well as limited amount of the samples.

The present research was supported by the Grant-in-Aid for Scientific Research No. 70000575 from the Ministry of Education, Science, Sports and Culture. The author (E. Fujimori) expresses his thanks to the Japan Society for Promotion of Science for the Research Fellowship for Young Scientists.

References

1) A. L. Gray, "Application of Inductively Coupled Plasma Mass Spectrometry," ed by A. R. Date and A. L. Gray, Blackie Academic & Professional, Glasgow (1989), Chap. 1.

2) K. E. Jarvis, A. L. Gray, and R. S. Houk, "Handbook of In-

ductively Coupled Plasma Mass Spectrometry," Blackie Academic & Professional, Glasgow (1992).

3) E. H. Evans and J. J. Giglio, *J. Anal. At. Spectrom.*, **8**, 1 (1993).

4) D. R. Wiederin, R. E. Smyczek, and R. S. Houk, *Anal. Chem.*, **63**, 1626 (1991).

5) Z. Peng, H. Klinkenberg, T. Beeren, and W. Van Borm, *Spectrochim. Acta, Part B*, **46B**, 1051 (1991).

6) M. Viczián, A. Lásztity, X. Wang, and R. M. Barnes, *J. Anal. At. Spectrom.*, **5**, 125 (1990).

7) K. K. Falkner and J. M. Edmond, *Anal. Chem.*, **62**, 1477 (1990).

8) J. H. Aldstadt, J. M. Kuo, L. L. Smith, and M. D. Erickson, *Anal. Chim. Acta*, **319**, 135 (1996).

9) J. R. Dean, L. Ebdon, H. M. Crews, and R. C. Massey, *J. Anal. At. Spectrom.*, **3**, 349 (1988).

10) G. H. Vickers, B. S. Ross, and G. M. Hieftje, *Appl. Spectrosc.*, **43**, 1330 (1989).

11) E. Fujimori, H. Sawatari, A. Hirose, and H. Haraguchi, *Chem. Lett.*, **1994**, 1467 (1994).

12) J. F. Tyson, *Analyst (London)*, **110**, 419 (1985).

13) A. G. Coedo and T. Dorado, *J. Anal. At. Spectrom.*, **10**, 449 (1995).

14) D. R. Lide, "CRC Handbook of Chemistry and Physics," 71st ed, CRC Press, Florida (1990).

15) E. Fujimori, H. Sawatari, K. Chiba, and H. Haraguchi, *Anal. Sci.*, **12**, 465 (1996).

16) A. Ando, T. Okai, Y. Inouchi, T. Igarashi, S. Sudo, K. Marumo, S. Itoh, and S. Terashima, *Bull. Geol. Surv. Jpn.*, **41**, 27 (1990).

17) S. Itoh, S. Terashima, N. Imai, H. Kamioka, N. Mita, and A. Ando, *Bull. Geol. Surv. Jpn.*, **43**, 659 (1992).

18) K. Toyoda and H. Haraguchi, *Bull. Chem. Soc. Jpn.*, **60**, 933 (1987).